J. Membrane Biol. 11, 377 – 398 (1973)

Solvent Drag by Solute-Linked Water Flow

A Theoretical Examination

S. Stender, K. Kristensen, and E. Skadhauge*

Institute of Medical Physiology, Dept. A,
University of Copenhagen, Denmark

Received 28 July 1972

Summary. Urea added to the outside of toad skin bathed in Ringer's solution increases the permeability of the skin to urea and sucrose, and creates a net inward flow of sucrose with a flux ratio of 3 to 4. Two hypotheses aim at explaining the sucrose transport, the first as entrainment in an inwardly directed water flow (anomalous solvent drag) created by urea (driving species) diffusion in the lateral intercellular spaces, the second as a direct solute-solute interaction.

The anomalous solvent drag model was formulated mathematically and simulated on an analogue computer. This permitted quantitative examination of the model assumptions and predictions. The flux ratio for the driven species (sucrose) was a function of two dimensionless parameters including the geometrical restrictions on the intercellular spaces, concentration of driving species, and diffusion coefficient of driving and driven species. For a range of experimental values of the system parameters, the calculated flux ratios of driven species were in agreement with most experimental findings. The unilateral fluxes would have to be restricted to 10^{-3} to 10^{-4} of the simple skin area. The ratio between the sucrose and urea flux ratios predicted by the model was equal to the observed value.

The solute-solute interaction model requires a coupling coefficient of 10^{-3} to account for the observed flux ratio. It is concluded that the anomalous solvent drag model is compatible with the bulk of experimental evidence available, whereas solute-solute interaction as occurring in free diffusion is far from being quantitatively sufficient.

An important problem in epithelial transport is how the flow of one species causes translocation of other species. Calculations of two types of interaction will be presented in this paper: solvent drag by solute-linked water flow and direct solute-solute interaction. Our theoretical considerations were prompted by the following experimental results.

* *Mailing address:* Institute of Medical Physiology A, 28 Juliane Mariesvej, 2100 Copenhagen, Denmark.

Hypertonicity with urea on the outside of a toad or frog skin bathed in Ringer's solution and with a tracer solute (sucrose) in equal concentration on both sides will result in an increase of permeability of the tracer solute in both directions, and furthermore a net transport in the inward direction, opposite to that of the net osmotic water flow. (Ussing, 1966; Franz & van Bruggen, 1967; Biber & Curran, 1968; Ussing & Johansen, 1969). This apparently active transport of the tracer solute has been shown to take place in cyanide-, dinitrophenol-, and ouabain-poisoned frog skins, suggesting that a metabolic process is not directly involved (Franz, Galey & van Bruggen, 1968).

In the so-called anomalous solvent drag model (ASD), Ussing (1969) suggested that this deviation of the sucrose permeability ratio from unity might be due to entrainment of sucrose molecules in a local water flow between the cells in the inward direction, created by urea diffusion into the intercellular spaces (IS). Alternatively, Biber and Curran (1968) suggested that the net flux of sucrose might arise as a result of "frictional" interaction with the urea diffusing across the skin due to the concentration difference.

We shall describe a simplified mathematical model of the ASD hypothesis, calculate some of its properties, and compare these with the relevant anatomical and physiological findings. The quantitative requirements of the solute-solute interaction model will also be considered.

Quantitative Description of the ASD Model

The hypertonic agent (the driving species, urea) is considered to pass the skin only through the IS, since the cell membrane has been found to be rather impermeable to urea (Ussing, 1969). It is assumed that this also is the case for the walls of the IS. Once in the IS, the urea will increase the osmolality of the IS and therefore draw water from the cells. The majority of this water will escape towards the inside since the basilar slit offers a much lower hydraulic resistance than the "tight junction" even rendered untight by the hypertonicity. As a consequence of these differences in hydraulic permeability directing water to the inside, hydraulic water flow across the tight junction is assumed negligible. This is also the case for diffusional water flow due to negligible water gradient. The tight junction is assumed not to be a hindrance to diffusion of small molecules like sucrose, urea or water (Ussing, 1969).

The driving solute will move towards the bathing solution at the open end of the channel as a result of diffusion and because it is being swept

along in the water stream. The water lost by the cells along the entire length of the IS will be replenished by osmosis through the basal – not the outer – cell membrane, since the basal has a considerably higher water permeability than the outer membrane (*see* Discussion of Assumptions of the Model). For similar reasons, the cell can be assumed to have an only slightly larger osmolality than the inside solution.

The local intercellular backflow of water takes place at the same time as a net water flow proceeds through the cells in the outward direction. In the steady state, a kind of standing gradient osmotic flow will be established in the IS (Diamond & Bossert, 1967). The backflow of water will augment diffusion of sucrose (driven species) in the direction of the flow, and impede diffusion in the opposite direction. This is the basis for the net transport of driven species according to the ASD model.

An important evidence for this recirculation model is that it has been possible to stop the net transport of sucrose by applying hydrostatic pressure to the inside of the skin without decreasing transport of the driving species, urea (Ussing & Johansen, 1969).

List of Parameters

IS	lateral intercellular space
TJ	"tight" junction
L	length of IS (μ)
A_E	epithelial surface area (μ^2)
S/A	circumference cross-section area ratio of the IS (μ^{-1})
n	total number of IS in area A_E
P_{os}	water permeability coefficient of lateral walls of IS ($\mu \times \sec^{-1} \times \text{osM}^{-1}$)
z, n, y, f, r	indices denoting driving species, NaCl, driven species, forward and reverse, respectively
in, out, cell	indices denoting inside, outside and cell, respectively
D	diffusion coefficient ($\mu^2 \times \sec^{-1}$)
C	concentration (osmolality, osM)
V	velocity of water in IS ($\mu \times \sec^{-1}$)
J	flux through the IS ($\text{osmol} \times \text{cm}^{-2} \times \sec^{-1}$)
P	permeability of the IS ($\text{cm} \times \sec^{-1}$)
P_E	permeability of epithelium ($\text{cm} \times \sec^{-1}$)
R	flux ratio (permeability ratio) $= P_f/P_r = P_{fE}/P_{rE}$

Mathematical Formulation of the ASD Model

With reference to assumptions leading to the physical model, as outlined in the preceeding section and Fig. 1, the following equations can be formulated: Conservation of mass (flux) in steady state of driving species through IS (due to diffusion and convection) requires:

$$J_z = -D_z \frac{dC_z}{dx} + V(x) C_z(x); \tag{1}$$

of bathing medium (NaCl):

$$J_n = -D_n \frac{dC_n}{dx} + V(x) C_n(x); \tag{2}$$

of driven species, unidirectional flux forward (inward) and reverse (outward) denoted f and r:

$$J_{yf} = -D_y \frac{dC_{yf}}{dx} + V(x) C_{yf}(x); \tag{3a}$$

$$J_{yr} = -D_y \frac{dC_{yr}}{dx} + V(x) C_{yr}(x); \tag{3b}$$

where $J_{z,n,y}$ flux of solute species are constant along the length of the IS since solutes are not transported across the lateral IS walls. (Note that J_{yr} will be negative in this notation.) D are diffusion coefficients, $C(x)$ solute concentrations, and $V(x)$ solvent linear velocity equal to solute velocity. Driven species, Eq. (3a) forward, (3b) reverse, are kept separate since they are separately measured with tracers.

Assuming semipermeability of the IS lateral walls and osmotic coefficients of unity, and neglecting solute partial molar volumes and hydro-

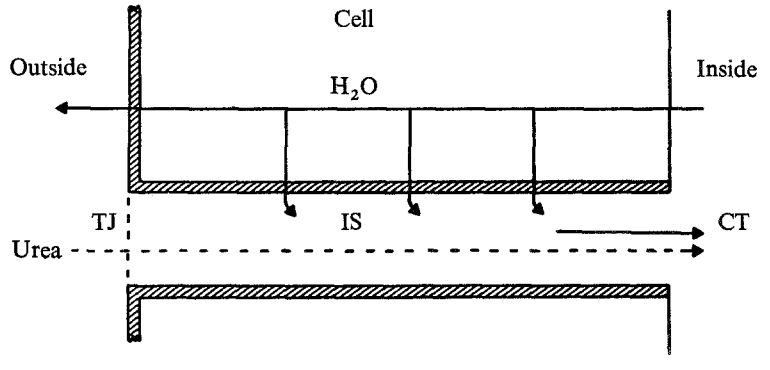

Fig. 1. The anomalous solvent drag model. Urea diffuses through the tight junction (TJ) into the lateral intercellular space (IS) and drags water osmotically from the cell into the IS. This water escapes through the basilar slit augmenting diffusion of molecules in the direction of flow, impeding diffusion in the opposite direction

static pressure, conservation of solvent (water) mass in steady state requires:

$$\frac{dV}{dx} = P_{os}\frac{S}{A}\left(C_z(x) + C_n(x) - C_{cell}\right) \tag{4}$$

where P_{os} denotes osmotic permeability coefficient of the IS walls, S/A the circumference to cross-section area ratio of the IS, C_z and C_n, osmotic concentration of driving species and NaCl, respectively, and C_{cell} the osmolality of the cell. The osmotic activity of driven species, "tracer solute," does not appear because of its insignificant (less than 1%) numeric contribution to osmolality.

The following boundary conditions as derived from the physical model are relevant: Concentrations just behind (to the right of) the TJ, $x=0$ are (almost) equal to outside concentrations in accordance to the section entitled Quantitative Description of the ASD Model, where TJ is assumed not to be a hindrance to diffusional transport of the involved molecules (as justified in the section entitled Discussion of Assumptions of the Model):

$$C_z(0) \cong C_{z\,out} \tag{5a}$$

$$C_n(0) \cong C_{n\,out} \tag{5b}$$

$$C_{yf}(0) \cong C_{y\,out} \tag{5c}$$

$$C_{yr}(0) \cong 0. \tag{5d}$$

There is a negligible solvent flow since TJ is assumed to have a much higher hydraulic resistance than both IS and basilar slit:

$$V(0) \cong 0. \tag{5e}$$

Just left of connective tissue (CT), $x=L$ concentrations are equal to inside concentrations:

$$C_z(L) \cong C_{z\,in} = 0 \tag{6a}$$

$$C_n(L) \cong C_{n\,in} = C_{n\,out} \tag{6b}$$

$$C_{yf}(L) \cong 0 \tag{6c}$$

$$C_{yr}(L) \cong C_{y\,in} = C_{y\,out}. \tag{6d}$$

For discussion of tight junction as well as connective tissue properties *see below.*

Computation of Solutions

The results of the model which have our main interest are the unidirectional flux or permeability ratios as well as the magnitude of the permeabilities themselves and the velocity of the solvent emerging from the IS inside

openings (basilar slits). Solutions of the system of Eqs. (1) through (4) with boundary conditions (5) through (6) were obtained partly by numerical (analogue simulation), partly by analytical methods (dimensional analysis). The analogue computation was carried out on an EAI 580 Analog/Hybrid Computing System simulating the appropriate scaled equations. Four feedback paths were implemented to guarantee the boundary conditions for $x=L$, Eqs. (6a–d). The values of the system variables at $x=L$ (or x) were obtained by sample/hold circuits.

It appears from dimensional analysis (Appendix A) that every dimensionless expression such as the flux ratio or the permeability taken relative to D/L fully is described by only two dimensionless parameters:

$$\beta=\frac{P_{os}\,S\,C_{z\,out}\,L^2}{AD_z}, \quad \text{and} \quad \frac{D_z}{D_y}, \tag{7}$$

assuming $C_{n\,in}=C_{n\,out}$ and D_n constant. L is length of IS. Note, that $C_{y\,in}$ and $C_{y\,out}$ do not appear directly as they have no osmotic effect. This means that within the descriptive framework of the model, every essential feature is determined only by these two dimensionless parameters (for a given bathing medium).

Flux (Permeability) Ratios

Standard solution of the differential Eqs. (3a) and (3b) applying the appropriate boundary conditions yield:

$$R_y=\frac{P_{yf}}{P_{yr}}=e^{+\frac{1}{D_y}\int_0^L V(x)\,dx} \tag{8}$$

or

$$\ln R_y=\ln\frac{P_{yf}}{P_{yr}}=\frac{1}{D_y}\int_0^L V(x)\,dx \tag{8a}$$

the right-hand side being determined by β and D_z/D_y only. The P's are IS permeabilities, which have the same ratio as the epithelial parameters P_E, because

$$P_E=P\frac{nA}{A_E} \tag{9}$$

n being the total number of IS for an epithelium area A_E, and A the IS cross-sectional area, the membrane considered isoporous for simplicity. Eq. (8) (derived by Koefoed-Johnsen & Ussing, 1953) could very easily be generalized to apply to both unidirectional permeability ratios for bathing NaCl and driving solute. In the latter case, driving species drives labeled

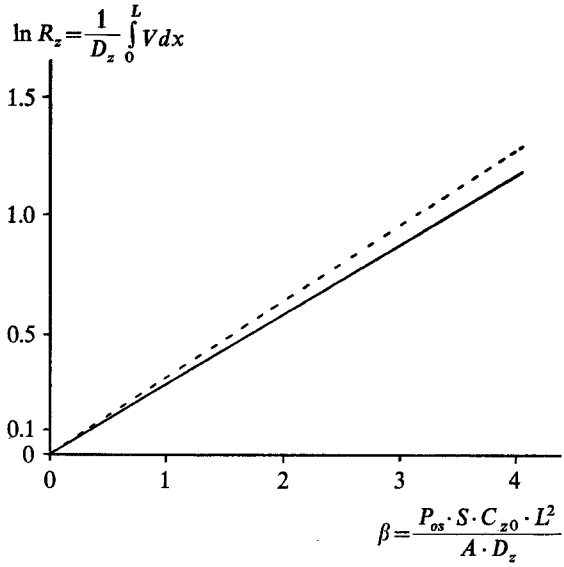

Fig. 2. Relation between flux ratio and the parameters of the system (selfdriving). The nondimensional parameter β is, within the range of biological interest, directly proportional to the natural logarithms of the flux ratio, which is proportional to the integrated water flow. The hatched line indicates the flux ratio resulting from a constant NaCl concentration in the IS

species of its own kind, selfdriving ($y=z$). In general:

$$\ln R = \ln \frac{P_f}{P_r} = \ln \frac{P_{Ef}}{P_{Er}} = \frac{D_z}{D} \frac{1}{D_z} \int_0^L V(x)\, dx \tag{8b}$$

with indices y, z, n suppressed. In case $y=z$ (selfdriving), Eq. (8b) reduces to Eq. (8a). Combining Eq. (8b) for different species, driven by the *same* driving species (D_z), yields:

$$\frac{\ln R_1}{\ln R_2} = \frac{D_2}{D_1}. \tag{8c}$$

The $\frac{1}{D_z} \int_0^L V(x) dx = \ln R_z$, selfdriving part of (8b) which is solely dependent on β is now to be determined.

In the relevant range of β (*see below*) analogue computation (Fig. 2, solid line) yields:

$$\frac{1}{D_z} \int_0^L V(x)\, dx \cong k \cdot \beta = 0.290 \cdot \beta. \tag{8d}$$

Consequently, Eq. (8b) can be rewritten:

$$\ln R = \ln \frac{P_f}{P_r} = \ln \frac{P_{Ef}}{P_{Er}} \cong 0.290 \cdot \beta \cdot \frac{D_z}{D} \tag{8e}$$

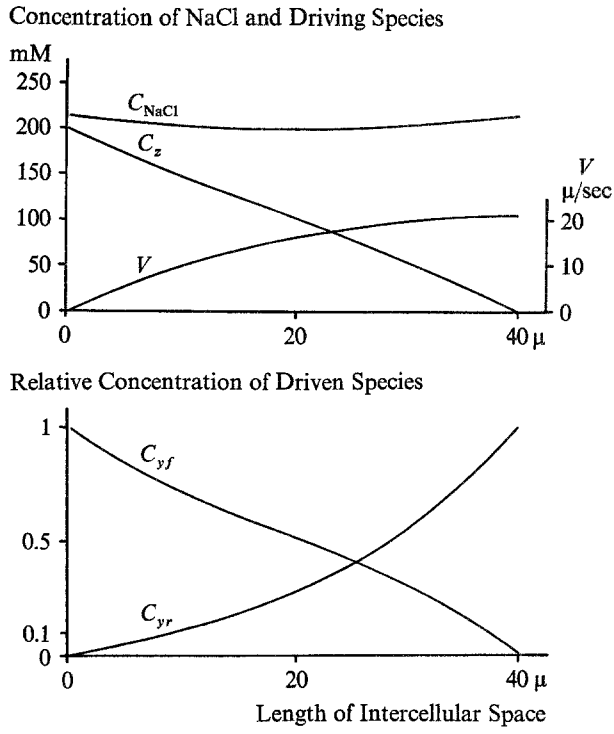

Fig. 3. Concentration profiles through the length of the intercellular space, and velocity of water flow. The driving species is urea of an outside concentration of 200 mM. Driven species is sucrose. The Ringer's solution is assumed to behave as NaCl. The case yielding a flux ratio for driven species of 3.6 is presented

with indices y, z, n. The hatched line in Fig. 2 corresponds to a constant NaCl concentration throughout the IS [Eq. (2) replaced with C_n=constant]. For the actual C_n profile, *see* Fig. 3 (typical case), from which it also is seen that NaCl might be omitted without considerable error.

Unidirectional Permeabilities

The IS permeabilities are taken relative to D/L, the IS permeabilities for zero solvent drag; i.e., $\frac{P}{D/L}$, which is a dimensionless expression. In accordance to the dimension analysis carried out, the expression is a function of β and D_z/D, D being D_z (selfdriving), D_y or D_n.

Analogue computation yields (Fig. 4) that forward permeabilities $\left(\frac{P}{D/L}>1\right)$ could be treated as linear with β in the relevant range (*see* Discussion), whereas reverse $\left(\frac{P}{D/L}<1\right)$ cannot, in accordance with Eqs. (8b, e).

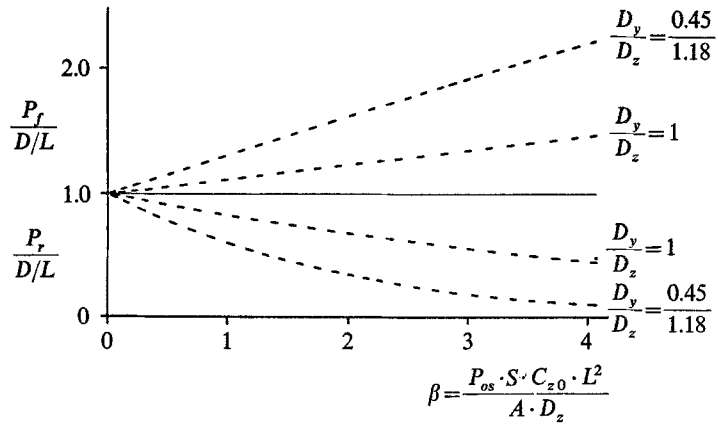

Fig. 4. Forward and reverse permeabilities as functions of solvent drag (β). The case for equal diffusion coefficients for driving and driven species (selfdriving) and the case for a diffusion coefficient ratio as in the urea-sucrose system are presented

It will be seen that this effect on the outflux and the influx is not symmetrical. Consequently,

$$\frac{P_{zf}}{D_z/L}\cong 1+0.115\cdot\beta. \tag{10a}$$

From analogue computation it can be verified that

$$\frac{P_{zf}-P_{yf}}{D_z/L-D_y/L}\cong 1.00 \tag{11}$$

within 0.01 or 1% in the relevant range of β and D_z/D_y ($\neq 1$).

Substituting (10a) in (11):

$$\frac{P_f}{D/L}\cong 1+0.115\cdot\beta\cdot\frac{D_z}{D};\quad z,y,n. \tag{10b}$$

For comparison with experiments, (10b) is rewritten to epithelial permeabilities Eq. (9):

$$P_{Ef}\cong\left(1+0.115\cdot\beta\cdot\frac{D_z}{D}\right)P_E^*, \tag{12a}$$

$$P_E^*=\frac{nAD}{A_E L};\quad z,y,n, \tag{12b}$$

P_E^* being the forward and reverse epithelial permeability corrected for the solvent drag effect. If Eq. (8e) is substituted in (12a),

$$P_{Ef}\cong(1+0.400\ln R)P_{Ef}^*;\quad z,y,n. \tag{12c}$$

Knowing the unidirectional permeabilities and consequently the flux ratio allows calculation of P_E^*.

Another version could be obtained by combining Eqs. (11) and (12b):

$$P_{Ezf} = \left(\frac{D_z - D_y}{D_y}\right) P_{Ey}^* + P_{Eyf}. \tag{12d}$$

Similar simple expressions could not be set up for reverse permeabilities. However, this is not necessary since Eqs. (8e) and (12a, b, c) contain sufficient information of the model, as visualized in Figs. 2 and 4.

Solvent Velocity

For estimation of recirculation of solvent (*see* Discussion):

$$\frac{V(L)_E}{P_E}\left(\beta, \frac{D_z}{D}\right); \quad z, y \tag{13}$$

was calculated. (z corresponds to urea and y to sucrose.) The magnitude of Eq. (13) was found to be around one and not exceeding two in the relevant β and D_z/D_y range. A typical velocity profile is shown in Fig. 3.

Comparison of Model Predictions and Experimental Results

It will now be examined whether the quantitative restrictions imposed by the model are compatible with the physiological and anatomical findings. Ideally, Eq. (8c)

$$\frac{\ln R_1}{\ln R_2} = \frac{D_2}{D_1}$$

should be tested by simultaneous use of two different kinds of driven species at the same skin or at paired halves with the same driving species. This is technically possible, but has not yet been performed.

In a similar way, Eq. (9) substituted in Eq. (11)

$$\frac{P_{Ezf} - P_{Eyf}}{D_z - D_y} = \frac{An}{LA_E}$$

might be tested, the right-hand side being a membrane constant.

The Relative Flux Ratio

From Ussing and Johansen (1969) we have taken the simple mean of the flux ratio of sucrose R_y and urea R_z measured before application of

hydrostatic pressure at different skins. We obtain

$$\frac{\ln R_y}{\ln R_z}=\frac{1.36}{0.49}=2.76$$

to be compared with

$$\frac{D_z}{D_y}=\frac{1.18}{0.4}=2.64$$

(diffusion coefficients at 20 °C and zero concentration). This good agreement should not be taken for more than a rough confirmation of Eq. (8c) because the calculation was based on eight different preparations.

Franz and van Bruggen (1967) have measured the changes in the flux ratios for four nonelectrolytes, urea, thiourea, mannitol and sucrose, on four different frog skins following the addition of 2.5% dimethylsulfoxide to the outer bathing solution. During the hypertonicity the flux ratio was found to be: 1.2 (thiourea), 2.6 (urea), 5.7 (mannitol) and 5.4 (sucrose). These four separately measured flux ratios cannot be used to a quantitative analysis considering the rather great variation in the responses of the individual skins. But it is at least in quantitative agreement with the model that mannitol and sucrose with low diffusion coefficients had higher flux ratios than thiourea and urea with higher diffusion coefficients.

The Absolute Flux Ratio

To yield a flux ratio of sucrose (1.32 to 4.8) and urea (1.2 to 2.0) as found by Ussing and Johansen (1969), the values of $\beta=\frac{P_{os}SC_{z\,out}L^2}{AD_z}$ must, according to Fig. 2 and Eq. (8e), be between 0.5 and 2.5 for the urea measurements and between 1.5 and 2.0 for the sucrose measurements.

The IS parameters as encountered experimentally in toad skin are as follows: The osmotic water permeability of the toad skin has been measured to be about $0.4\,\mu\times\sec^{-1}\times\mathrm{osM}^{-1}$ (Kofoed-Johnsen & Ussing, 1953; Whittenbury, 1962). This value may be considered a guide of the water permeability of the lateral cell walls. We therefore employ a range of P_{os}: 0.1 to $1.0\,\mu\times\sec^{-1}\times\mathrm{osM}^{-1}$. L: approximately 40 μ. $S/A=2/b$, when considering a narrow slit with the width b. b: 0.1 to 1.0 μ giving a range for β of 0.05 to 10 when $D_z=1.18\times10^3\,\mu^2\times\sec^{-1}$ (International Critical Tables) and $C_{z\,out}=0.2$ osM. Since the experimental values of β are within this range, it may be concluded that the flux ratios observed experimentally are quantitatively possible within the framework of the ASD model.

Urakabe, Handler and Orloff (1970) have performed experiments on the toad (*Bufo marinus*) urinary bladder, a tissue which has many physio-

logical properties in common with frog skin. After addition of 240 mM urea to the mucosal side, a shunt pathway was probably opened since the electric resistance fell and the sucrose permeability went up from 20×10^{-8} cm $\times$ sec^{-1} to 80 but without the flux ratio deviating significantly from unity. Since ln R_y varies with the second power of L [Eq. (8e)] the absence of deviation of sucrose flux ratios from unity might be due to the thinness (approx. 10 μ) of the urinary bladder assuming S/A and P_{os} to be the same as in toad skin. If typical toad skin values with a flux ratio of 4 for a length of 40 μ is changed to 10 μ the flux ratio *ceteris paribus* becomes 1.09, which experimentally cannot be distinguished from unity.

Relative Permeability

The unidirectional permeabilities P_E^* for sucrose and urea in the case of no flow of water in the IS, have been calculated using Eq. (12c) on Ussing and Johansen's (1969) data. P_E^* for sucrose varies between (32 and 42) $\times 10^{-8}$ cm $\times$ sec^{-1} and for 4 other skins P_E^* for urea were 3.5 to 10 times higher.

According to the model, the permeabilities due only to diffusion of the solutes through the same skin should be related by the ratio of their diffusion coefficients, in this case $D_z/D_y = 2.64$. The discrepancy may be due to two factors. First, the values of P_{Ez}^* and P_{Ey}^* originate from different skins reducing their comparability. Second, the fact that P_{Ez}^*/P_{Ey}^* is higher than D_z/D_y suggests an alternative pathway for urea (intracellular) as mentioned by Ussing and Johansen (1969).

From (12b) it follows that $\frac{An}{A_E} = \frac{P_E^* L}{D}$. For the estimated range of L the range of $\frac{An}{A_E}$ is 0.7×10^{-3} to 0.7×10^{-4}. The requirements to the IS in a membrane yielding the unidirectional permeabilities P_{Ef} and P_{Er} are then:

$$\ln \frac{P_{Ef}}{P_{Er}} \cong 0.29 \cdot \beta \cdot \frac{D_z}{D} \tag{8e}$$

$$\frac{An}{A_E} = \frac{P_E^* L}{D}. \tag{12b}$$

If β is 1.4 (flux ratio 4) and $C_{z\,out}$ is equal to 200 mosM in a toad skin epithelium of a thickness of 40 μ, P_{os}/b must be 10. With P_{os} in the range of 0.4 to 4 μ $\times$ sec^{-1} $\times$ osM^{-1}, this requirement can be met by a slit width of 0.04 to 0.4 μ. For $L = 40$ μ the $\frac{An}{A_E}$ —assuming free diffusion— will, according to Eq. (12b), be 0.3×10^{-3}. Given a slit width of 0.04 to 0.4 μ and

an epithelial cell "diameter" of 10 to 20 μ it can be estimated how large a fraction of the possible IS area actually is exhibiting solvent drag characteristics: Area per cell: 100 to 200 μ^2. Maximal possible slit area per cell assuming slits all around the cell (4 per cell shared with 4 surrounding cells equal to 2 full slits): 0.8 to 16 μ^2. The resulting maximal possible fractional slit (IS) area is 0.4×10^{-2} to 1.6×10^{-1} to be compared with $\frac{nA}{A_E}$ in the order of 0.3×10^{-3}. The estimated fraction ranges from 0.2 to 7.5%.

Effects on Epithelial Permeabilities Caused by Increased Outside Hypertonicity

The permeability of sucrose in the absence of urea hypertonicity and therefore in the absence of solvent flow in the IS have been measured to only about 3×10^{-8} cm $\times$ sec^{-1} (Ussing & Johansen, 1969). Assuming that the number n of IS and the length L are independent of $C_{z\,\mathrm{out}}$, the concentration of driving species, it follows from Eq. (12b) that

$$\frac{A_{0.2}}{A_{0.0}} = \frac{(P_E^*)_{0.2}}{(P_E^*)_{0.0}} = 10$$

where the indices 0.0 and 0.2 indicate the concentration of driving species.

The suggestion that the cross-section area A of the IS increases with increasing concentration of driving species seems to be in good agreement with the model since the kinetics implies a hydrostatic pressure in the IS which distend the IS. A cell shrinkage due to the outside hyperosmolality may also increase the IS area. Such shrinkage has been observed by Erlij and Martinez-Palomo (1972).

Biber and Curran (1968) have investigated how the influx and efflux of mannitol through a toad skin varies with the urea hypertonicity. They have found both fluxes to increase almost linearly when the urea concentration increases, but the slope was much steeper for the influx, resulting in an almost linear relationship between the flux ratio for mannitol and the urea concentration. This is at first sight not in accordance with the exponential relationship predicted by the ASD model [Eq. (8e)]. Since the IS area increases (S/A decreases) with increasing urea concentration, the flux ratio for mannitol, however, increases more slowly.

In Fig. 5 the directly observed mannitol permeabilities have been plotted against the urea concentration with data from Fig. 3 in Biber and Curran (1968). Using Eq. (12c) the solvent drag effect on mannitol has been eliminated and the P_E^* has been calculated. According to Eq. (12b)

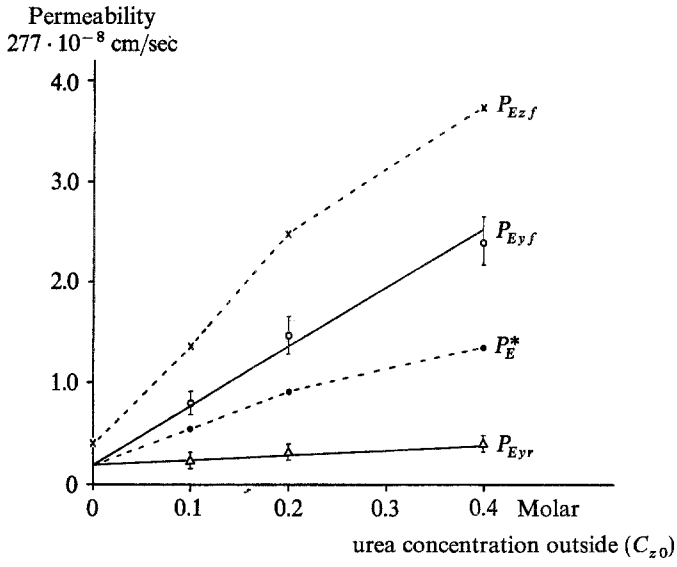

Fig. 5. A calculation of the epithelial permeability of driven species as a function of concentration of driving species including varying IS area. The data for the urea mannitol system from Fig. 3 in Biber and Curran (1968) have been used. The open circles and triangles indicate observed mannitol permeabilities in the inward and outward direction. The closed circles indicate the mannitol permeability corrected for solvent flow according to the anomalous solvent drag model. The crosses indicate the resulting urea permeability

the change in P_E^* is due to the increase in IS area (larger slit width b) caused by the increased urea concentration. The area increase (4 times) is thus quantitatively comparable with the increase (10 times) estimated from the driven species permeability in Ussing and Johansen's (1969) experiments. The difference may be due to differences in equilibration periods used by the investigators.

The increase in IS area may explain why the relationship between urea concentration and influx and efflux of mannitol is almost linear over the observed range. The efflux increases due to the increased area. This increase is smaller than for the influx because it is against the solvent flow. This is not as large as it would have been for the urea concentration used if the area had not increased. The inward permeability for urea has, in Fig. 5, been calculated according to Eq. (12d) or Fig. 4.

On the basis of Fig. 5 the influx of mannitol has been depicted explicitly as a function of the calculated urea influx. Over the given range the relationship appears to be a power function with power less than unity (Fig. 6).

It will thus be seen that taking the experimental variation into account, an observed "linear" relationship between the two fluxes, would not be

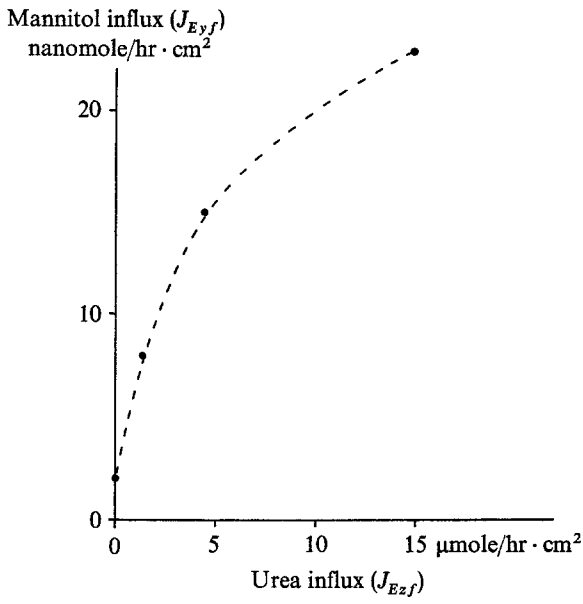

Fig. 6. A calculation of the relation between influx of driving and driven species as predicted by the anomalous solvent drag model. The points are based on Biber and Curran's (1968) data as calculated in Fig. 5

incompatible with the ASD model considering the concentration dependent area increase.

Based on the solute-solute interaction model, Biber and Curran (1968) predict a linear relationship between the two fluxes. A single experiment has been taken to support this concept (Fig. 4), although a power function would fit the experimental points with equal right. Fig. 4 is, however, not comparable with our Fig. 6 and Biber and Curran's own Fig. 3, since in Fig. 4 the mannitol flow per millimolar urea on the outside is only $\frac{1}{10}$ to $\frac{1}{2}$ (depending on concentration) of the flow in Fig. 3. This may explain why the absolute values of Fig. 4 do not give reasonable results using Eq. (12d).

Discussion of Assumptions of the Model

Recycling of Solvent Flow

How large a fraction of the transepithelial water flow is recirculating through the lateral walls of the IS? According to the model this could be estimated using Eq. (13). For a typical sucrose permeability P_{Eyf} of 50×10^{-8} cm $\times$ sec^{-1} the epithelial water flux, equal in magnitude to epithelial

linear velocity:

$$\frac{V(L)nA}{A_E} \cong \frac{2P_{yf}nA}{A_E} = 2P_{Eyf}$$

$$= 10^{-6}\,\text{cm} \times \text{sec}^{-1} = 3.6\ \mu\text{liters} \times \text{cm}^{-2} \times \text{hr}^{-1}.$$

Franz and van Bruggen (1967) have measured the net water outflux during 200 mOsm mannitol hypertonicity to be 20 μliters $\times$ cm^{-2} $\times$ hr^{-1}, the recycling water flux thus only being a fraction thereof. The recycling water flux when entering from inside to the cell requires a certain transmembrane osmotic difference permeability product.

The effect of the hypertonicity of the IS on the cell concentration has been neglected in the following estimates. This is permissible according to the estimates in the section entitled Comparison of Model Predictions and Experimental Results, Relative Permeability, that only a fraction of possible IS (max. 7%) needs to be functioning to account for the observed flux ratio. This is not the case in the model of Lindemann and Pring (1969) treating water following actively transported NaCl.

Given a reasonable estimate of osmotic difference, negligible in accordance to assumption $C_{\text{cell}} \cong C_{\text{in}}$, will the resulting inside permeability be reasonable? A tentative osmotic difference of 10 mosM would require a P_{os} of 10^{-4} cm $\times$ sec^{-1} $\times$ osM^{-1} or 1 $\mu \times$ sec^{-1} $\times$ osM^{-1}. On frog skin, the permeability coefficients have been estimated both for the outside and the inside of the same skin (MacRobbie & Ussing, 1961). The inside permeability was 25 times larger than the outside permeability by a maximum estimate of the outside and a minimum estimate of the inside permeability.

Some support for considering the outside permeability much smaller than inside permeability also in toad skin is found in the finding of identical permeability coefficients for whole skin and for the outer membrane: They have both been estimated to 24 $\mu \times$ sec^{-1} $\times$ osM^{-1} (Koefoed-Johansen & Ussing, 1953; Whittenbury, 1962; Franz & van Bruggen, 1967). Thus, recycling of solvent does not invalidate the assumption: $C_{\text{cell}} \cong C_{\text{in}}$, given reasonable estimates of "inner" P_{os}.

Hydrostatic Pressure in the IS

Calculations of the hydrostatic pressure fall, integrated along the length of the IS, from the water flow and reasonable dimensions of the IS yield hydrostatic pressures less than 1 cm H_2O at $x=0$. This pressure, obtained under the assumption of negligible water movement across the TJ, conse

quently represents a maximum estimate, which safely could be used to estimate hydraulic flow across TJ. If a 1-cm H_2O pressure difference is applied across a TJ of 0.05-μ length consisting of circular pores of 0.001-μ radius of a total area of 5% of the IS area, the water flow will be about 0.5×10^{-3} of the $V(L)$. This negligible flow will impede diffusion of solutes across the TJ by less than 1%. These calculations justify the boundery conditions chosen. The equivalent pore radius of the TJ is quite well estimated by the physiological evidence, since the skin is impermeable to inulin (radius 0.0015 μ).

It is possible to speculate that a significant backflow of water may occur across the TJ if the IS pressure is increased to 25 cm H_2O, and may in this way abolish the net transport of sucrose but not the urea flow (Ussing & Johansen, 1969).

Concentration Difference Across TJ Resistance

In the above calculations, the TJ was assumed to have a zero concentration difference. Knowing the approximate length area ratio of TJ and IS, it can be estimated how large a fraction of total (inside to outside) concentration fall occurs over the TJ.

Solute transport resistance (in steady state) is proportional to L/A, in IS being modified by the flow by a factor less than two.

$$\text{For IS: } \left(\frac{L}{A}\right)_{IS} \sim \frac{40\mu}{1\mu^2} = 40\mu^{-1}.$$

$$\text{For TJ: } \left(\frac{L}{A}\right)_{TJ} \sim \frac{0.05\mu}{0.05\mu^2} = 1\mu^{-1}.$$

As transport resistance of a typical TJ is in the order of 2% of IS it could safely be neglected.

For these calculations the TJ area was assumed to be 5% of the IS area, and a length of TJ of 0.05 μ was used, since it has been observed from around 0.02 to around 0.2 μ (Farquhar & Palade, 1965; Martinez-Palomo, Erlij & Bracho, 1971).

Concentration Difference Across Connective Tissue (CT)

Due to the

$$\left(\frac{L}{A}\right)_{CT} = \frac{160\mu}{1000\mu^2} = 0.16\mu^{-1}$$

(typical, calculated per functioning IS) being a negligible fraction of the $(L/A)_{IS}$, the concentration difference over connective tissue could be disregarded in the steady state. This is not the case in nonsteady state due to the large solute distribution volume.

The Solute-Solute Interaction Model

Biber and Curran (1968) considered a direct coupling between driving and driven species without invoking a solvent flow. They calculated within the framework of irreversible thermodynamics the coupling coefficient (expressed as a mobility) (ω_{u-m}) for the urea (u)-mannitol (m) system. The mannitol flux ratio appears from the following equation:

$$\frac{J_{m\,0-i}}{J_{m\,i-0}} = \frac{P_m C_m + \frac{\omega_{m-u}}{\omega_u} J_u}{P_m C_m - \frac{\omega_{m-u}}{\omega_u} J_u}. \tag{14}$$

If the unilateral fluxes (J_m), the urea flow (J_u) and the urea mobility (ω_u), or permeability, are measured, the coupling coefficient can be calculated and the coupling ratio $\frac{\omega_{m-u}}{\omega_u}$ found. (Note that the ω_{m-u} in this notation is proportional to the mannitol concentration, as intuitively clear. Otherwise the flux ratio would vary with the chemical concentration of mannitol.) Calculated in this way, the coupling ratio will, according to Fig. 3 in Biber and Curran (1968), be 2.5×10^{-3}, according to the data in Ussing and Johansen (1969) for the urea sucrose system 1.8×10^{-2}. For both calculations, a urea permeability at 200 mM urea outside of 0.01 cm/hr was assumed. Biber and Curran note that coupling ratios as large as 0.1 have been observed in free diffusion experiments with ions. Since the observed degree of coupling, however, is extremely dependent upon the molecules involved, larger for ions, and the experimental conditions, membrane experiments rather than free diffusion experiments might be used for comparison. Galey and van Bruggen (1970) have performed experiments on artificial membranes with pore sizes of 350, 80 and 20 Å and used mannitol, sucrose and raffinose as solutes. These workers observed coupling ratios up to 10^{-3}. These experiments were, however, done with net water flow prevented by hydrostatic pressure. In this system membrane inhomogeneity may, according to Patlak and Rapoport (1971), account for the coupling. Thus, the true coupling ratio for this system is probably much lower than 10^{-3}.

The coupling ratio measured in free diffusion experiments with the Gouy diffusiometer also deserves scrutiny. In ternary diffusion experiments, the coupling ratios are almost directly proportional to the concentration of the driven species. This observation has been made for the raffinose-KCl system (Dunlop, 1957), for the NaCl–KCl system (Fujita & Gusting, 1960) and for the sucrose-mannitol system (Ellerton & Dunlop, 1967*a*). For the urea-sucrose system, Ellerton and Dunlop (1967*b*) reported a coupling ratio of 0.002:0.911 ($\times 10^{-5}$ cm$^2 \times$ sec^{-1}) for equal solute concentrations of 0.5 moles per liter. If the sucrose concentration is 10^{-2} of the urea concentration, the coupling ratio will thus be expected to be about 2×10^{-5}. This leaves a really large distance to the coupling ratio of 10^{-2} required to explain the flux ratio as observed by Ussing and Johansen (1969). The conclusion thus seems to be that solute-solute interaction alone cannot account for the experimental findings unless "single file" phenomena occur in the TJ resulting in higher coupling coefficients.

General Discussion

Three possibilities exist: (1) The hypotheses offered so far may have little connection to the events occurring in epithelial tissues, (2) either anomalous solvent drag, or (3) solute-solute interaction may be quantitatively most important. Theoretical model calculations can never rule out the first possibility, but they can quantitate the limits of the models. The anomalous solvent drag model seems to survive quantitative scrutiny. It was found compatible with the majority of the biological findings. The relationship between permeability and flux ratio for molecules of different diffusion coefficients seems compatible with model predictions and should be open to further investigation. The experimentally weakest points of the model are the relative ignorance of the exact nature of the tight junctions. Furthermore, since the ASD model is so dependent upon length of the IS, both stratum granulosum and germinativum must be assumed to participate.

The solute-solute interaction model does not seem quantitatively sufficient if interaction coefficients as small as in free diffusion experiments apply. It remains to be determined whether special interactions such as "single file" diffusion occur in membranes similar to the tight junctions in the absence even of local solvent flows.

In a "reversed" experiment (urea added to inside) Biber and Curran (1968) have reported a flux ratio deviating significantly from unity, although the tracer fluxes were only about one-tenth of those observed in the "forward" experiment. Within the assumptions of the anomalous solvent drag

model reverse bulk flow is not possible, and consequently cannot account for flux ratios deviating from unity. The "reversed" observations might be due to solute-solute interaction with its considerably lower coupling. The net flow of urea should be measured in such experiments.

As a general biological principle, solvent drag due to solute-linked water flow deserves interest. Given reasonable differential permeabilities, local osmotic water flows, as originally suggested by Curran (1960), may be important in renal and intestinal epithelia. Urea has been suggested to drive sodium in mammalian kidney (Ussing, 1969), and sodium may drive urea in elasmobranch kidney (Schmidt-Nielsen, Truniger & Rabinowitz, 1972), and in intestine glucose may drive sodium, or vice versa.

It is a pleasure to thank Professor Hans H. Ussing for continued interest and stimulating discussions during the prosecution of this work. The analogue computer was supported by The Danish Medical Research Council.

Appendix A

The system of Eqs. (1) through (4) and set of boundary conditions (5) through (6) determine the model completely. This description includes for the selfdriving case the following six parameters: S, A, L, P_{os}, D_z, $C_{z\,out}$. Every dimensionless expression such as $R_z = P_{zf}/P_{zr}$ or $P_{zf}/D_z/L$ is solely dependent on these six parameters in dimensionless combination.

To find these combinations we proceed (Bridgman, 1922; Segel, 1970): P_{os}, S and A appear in Eq. (4) as $P_{os}S/A$. The latter together with L, D_z and $C_{z\,out}$ are combined in powers:

$$\left(\frac{P_{os}\,S}{A}\right)^{a_1} \cdot (C_{z\,out})^{a_2} \cdot (D_z)^{a_3} \cdot (L)^{a_4}. \tag{A.1}$$

Insertion of dimensions length L, mass M and time T and rearranging yields:

$$M^{-a_1+a_2} \cdot L^{3a_1-3a_2+2a_3+a_4} \cdot T^{-a_1-a_3} \tag{A.2}$$

which should be dimensionless requiring zero powers: $(-a_1+a_2=0)$ and $(3a_1-3a_2+2a_3+a_4=0)$ and $(-a_1-a_3=0)$. A solution is: $a_1=x$, $a_2=x$, $a_3=-x$ and $a_3=2x$, x being arbitrary. When inserted in (A.1):

$$\left(\frac{P_{os}\,S\,C_{z\,out}\,L^2}{AD_z}\right)^x.$$

The simplest case $x=1$ yields β. For selfdriving only one parameter β is necessary. For the general case D_y is added. $C_{y\,in}$, $C_{y\,out}$ are not since

they are not osmotically active and $C_{n\,\text{in}} = C_{n\,\text{out}}$ are not since they are constant (Ringer's). In this case, another dimensionless parameter D_z/D_y is required. This could be seen directly [derivation of Eq. (8)] or by another dimensional analysis including D_y. Note that y could be interchanged with n.

References

Biber, T. U. L., Curran, P. F. 1968. Coupled solute fluxes in toad skin. *J. Gen. Physiol.* **51**:606.

Bridgmann, P. W. 1922. Dimensional Analysis. Yale University Press New Haven, Conn.

Curran, P. F. 1960. Na, Cl and water transport by rat ileum *in vitro*. *J. Gen. Physiol.* **43**:1137.

Diamond, J. M., Bossert, W. H. 1967. Standing-gradient osmotic flow. *J. Gen. Physiol.* **50**:2061.

Dunlop, P. J. 1957. A study of interacting flows in diffusion of the system raffinose-KCl-H_2O at 25°. *J. Phys. Chem.* **61**:994.

Ellerton, H. D., Dunlop, P. J. 1967*a*. Diffusion and frictional coefficients for four compositions of the system water-sucrose-mannitol at 25°. Tests of the Onsager reciprocal relation. *J. Phys. Chem.* **71**:1291.

Ellerton, H. D., Dunlop, P. J. 1967*b*. Ternary diffusion and frictional coefficients for one composition of the system water-urea-sucrose at 25°. A test of the Onsager reciprocal relation for this system. *J. Phys. Chem.* **71**:1538.

Erlij, D., Martinez-Palomo, A. 1972. Opening of tight junctions in frog skin by hypertonic urea solutions. *J. Membrane Biol.* **9**:229.

Farquhar, M. G., Palade, G. E. 1965. Cell junctions in the amphibian skin. *J. Cell. Biol.* **26**:263.

Franz, T. J., Bruggen, J. T. van. 1967. Hyperosmolarity and the net transport of non-electrolytes in frog skin. *J. Gen. Physiol.* **50**:933.

Franz, T. J., Galey, W. R., Bruggen, J. T. van. 1968. Further observation on asymmetrical solute movement across membranes. *J. Gen. Physiol.* **51**:1.

Fujita, H., Gosting, L. G. 1960. A new procedure for calculating the four diffusion coefficients of three-component systems from Gouy diffusiometer data. *J. Phys. Chem.* **64**:1256.

Galey, W. R., Bruggen, J. T. van. 1970. The coupling of solute fluxes in membranes. *J. Gen. Physiol.* **55**:220.

Koefoed-Johnsen, V., Ussing, H. H. 1953. The contribution of diffusion and flow to the passage of D_2O through living membranes. *Acta. Physiol. Scand.* **28**:60.

Lindemann, B., Pring, M. 1969. A model of water absorbing epithelial cells with variable cellular volume and variable width of the lateral intercellular gaps. *Pflüg. Arch. Ges. Physiol.* **307**:55.

MacRobbie, E. A. C., Ussing, H. H. 1961. Osmotic behaviour of the epithelial cells of frog skin. *Acta Physiol. Scand.* **53**:348.

Martinez-Palomo, A., Erlij, D., Bracho, H. 1971. Localization of permeability barriers in the frog skin epithelium. *J. Cell. Biol.* **50**:277.

Patlak, C. S., Rapoport, I. 1971. Theoretical analysis of net tracer flux due to volume circulation in a membrane with pores of different sizes. *J. Gen. Physiol.* **57**:113.

Schmidt-Nielsen, B., Truniger, B., Rabinowitz, L. 1972. Sodium linked urea transport by the renal tubule of the spiny dogfish *Squalus acanthias*. *Comp. Biochem. Physiol.* **42**A:13.

Segel, L. A. 1970. Standing-gradient flows driven by active solute transport. *J. Theoret. Biol.* **29**:233.

Urakabe, S., Handler, J. S., Orloff, J. 1970. Effect of hypertonicity on permeability properties of the toad bladder. *Amer. J. Physiol.* **218**:1179.

Ussing, H. H. 1966. Anomalous transport of electrolytes and sucrose through the isolated frog skin induced by hypertonicity of the outside bathing solution. *Ann. N. Y. Acad. Sci.* **137**:543.

Ussing, H. H. 1969. The interpretation of tracer fluxes in terms of membrane structure. *Quart. Rev. Biophys.* **1**:365.

Ussing, H. H., Johansen, B. 1969. Anomalous transport of sucrose and urea in toad skin. *Nephron* **6**:317.

Whittembury, G. 1962. Action of antidiuretic hormone on the equivalent pore radius at both surfaces of the epithelium of the isolated toad skin. *J. Gen. Physiol.* **46**:117.